



## Development and *in-vivo* characterization of supramolecular hydrogels for intrarenal drug delivery

Patricia Y.W. Dankers<sup>a,b,c,\*</sup>, Marja J.A. van Luyn<sup>a</sup>, Ali Huizinga-van der Vlag<sup>a</sup>, Gaby M.L. van Gemert<sup>d</sup>, Arjen H. Petersen<sup>a</sup>, E.W. Meijer<sup>b,c</sup>, Henk M. Janssen<sup>d</sup>, Anton W. Bosman<sup>e</sup>, Eliane R. Popa<sup>a</sup>

<sup>a</sup> Department of Pathology and Medical Biology, Stem Cells and Tissue Engineering Group, University of Groningen, University Medical Center Groningen, Hanzeplein 1, 9713 GZ Groningen, The Netherlands

<sup>b</sup> Institute for Complex Molecular Systems, Eindhoven University of Technology, P.O. Box 513, 5600 MB Eindhoven, The Netherlands

<sup>c</sup> Laboratory of Chemical Biology, Eindhoven University of Technology, P.O. Box 513, 5600 MB Eindhoven, The Netherlands

<sup>d</sup> SyMO-Chem BV, Den Dolech 2, 5612 AZ Eindhoven, The Netherlands

<sup>e</sup> SupraPolix Research Center, Horsten 1, 5612 AX Eindhoven, The Netherlands

### ARTICLE INFO

#### Article history:

Received 23 February 2012

Accepted 13 March 2012

Available online 9 April 2012

#### Keywords:

Animal model  
Biocompatibility  
Drug delivery  
Hydrogel  
*In vivo* test  
Tissue response

### ABSTRACT

Intrarenal drug delivery from a hydrogel carrier implanted under the kidney capsule is an innovative way to induce kidney tissue regeneration and/or prevent kidney inflammation or fibrosis. We report here on the development of supramolecular hydrogels for this application. We have synthesized two types of supramolecular hydrogelators by connecting the hydrogen bonding moieties to poly(ethylene glycols) in two different ways in order to obtain hydrogels with different physico-chemical properties. Chain-extended hydrogelators containing hydrogen bonding units in the main chain, and bifunctional hydrogelators end-functionalized with hydrogen bonding moieties, were made. The influence of these hydrogels on the renal cortex when implanted under the kidney capsule was studied. The overall tissue response to these hydrogels was found to be mild, and minimal damage to the cortex was observed, using the infiltration of macrophages, formation of myofibroblasts, and the deposition of collagen III as relevant read-out parameters. Differences in tissue response to these hydrogels could be related to the different physico-chemical properties of the three hydrogels. The strong, flexible and slow eroding chain-extended hydrogels are proposed to be suitable for long-term intrarenal delivery of organic drugs, while the weaker, soft and fast eroding bifunctional hydrogel is eminently suitable for short-term, fast delivery of protein drugs to the kidney cortex. The favourable biological behaviour of the supramolecular hydrogels makes them exquisite candidates for subcapsular drug delivery, and paves the way to various opportunities for intrarenal therapy.

© 2012 Elsevier Ltd. All rights reserved.

### 1. Introduction

The worldwide increasing incidence of end-stage renal disease raises the need for innovative therapeutic approaches that promote functional kidney regeneration, thereby preventing chronic renal failure. Current therapies include the systemic, i.e. intravenous or intraperitoneal, administration of anti-inflammatory, immune-suppressive and anti-fibrotic drugs. However, these strategies are accompanied by unwanted side effects due to lack of control over drug localization. Major progress has been made in the research of targeted drug delivery to for example proximal tubular epithelial

cells [1]. In this work we show a new approach consisting of the implantation of a drug delivery system under the kidney capsule. As carrier systems we use hydrogels that due to their physical properties are proposed to be able to adjust to the subcapsular space.

Many hydrogels have been used for regenerative medicine and drug delivery purposes [2,3], frequently by implantation or injection at various sites in the body. Detailed studies on the tissue response to different hydrogels mainly focus on subcutaneous implantation [4–6] while studies on subcapsular implantation remain limited. The kidney capsule as implantation site is primarily investigated for pancreatic cell or islets transplantation in diabetic animal models [7]. These cells have for example been encapsulated in microcapsules and their survival and function have been studied under the kidney capsule [8,9]. However, studies on the tissue response to subcapsularly implanted hydrogel systems, that are designed for intrarenal drug delivery, are to our knowledge not present.

\* Corresponding author. Institute for Complex Molecular Systems, Eindhoven University of Technology, P.O. Box 513, 5600 MB Eindhoven, The Netherlands. Tel.: +31 40 247 5620; fax: +31 40 247 8367.

E-mail address: [p.y.w.dankers@tue.nl](mailto:p.y.w.dankers@tue.nl) (P.Y.W. Dankers).

In this study we designed and synthesized three supramolecular hydrogels for use as intrarenal drug delivery systems and investigated the renal tissue response after subcapsular implantation. We use supramolecular hydrogels, i.e. hydrogels in which the network is formed by directed non-covalent interactions, so-called transient supramolecular networks. These supramolecular systems are proposed to have physical properties which allow for easy implantation between and adjustment to the renal capsule and the soft cortical kidney tissue. Recently, we have shown that supramolecular building blocks based on ureido-pyrimidinone (UPy) units [10] are excellent elastomeric biomaterials [11–13]. Also, bioactive supramolecular materials could be made by simple mixing of UPy-modified prepolymers and UPy-functionalized peptides [14,15]. In the past, the tissue response to these UPy-modified biomaterials have been studied subcutaneously [11,14,16,17]. Here, we apply this supramolecular and modular principle to design hydrogels by introduction of UPy-moieties on poly(ethylene glycol) (PEG) prepolymers. Recently we have published an extensive study on the properties of different telechelic UPy-modified PEGs [18]. Here, we show the difference between two types of PEG hydrogelators, containing UPy-moieties in the main chain **1** and **2**, or at the chain ends **3** (i.e. telechelic UPy-PEGs) (Fig. 1A). After discussing the synthesis, formulation procedure and rheological behaviour of these hydrogels, we report on their intrarenal behaviour and tissue response, and propose possible therapeutic applications in relation to their physical properties.

## 2. Materials and methods

### 2.1. Syntheses of UPy-modified hydrogelators

All syntheses were performed as described in the [supplementary information](#).

### 2.2. Preparation of hydrogels

UPy-polymer **1** was dissolved in THF (Biosolve) and a 0.9% NaCl (B. Braun Melsungen) aqueous solution was added in a ratio 1:1 to obtain a 5 w/w% hydrogel. The clear solution was subsequently put *in vacuo* to slowly remove the THF, resulting in a very elastic hydrogel. The same procedure was applied to UPy-polymer **2**, resulting in an elastic, rigid and shape-persistent 5 w/w% hydrogel. After preparation, gel **1** and **2** were incubated in a 0.9% NaCl solution for 16 h at 4 °C to ensure that all organic solvents were washed out. A 10 w/w% hydrogel of **3** was prepared by mixing the hydrogelator powder and a 0.9% NaCl aqueous solution in the appropriate loading ratio. The mixture was vigorously mixed by stirring at 55–65 °C for 1 h. The polymer solution was removed from the water bath and placed on the bench at 21 °C to set over a 16–24 h period, which resulted in a soft hydrogel. Subsequently, the gel could immediately be used. All gels were sterilized with UV for 1 h prior to use.

### 2.3. Rheology

For rheology measurements, 5 w/w% gel **1** and 10 w/w% gel **3** were heated and melted on the rheometer in order to be moulded into the proper shape for measurement. The samples were left to set for several hours before the measurements were performed. The 5 w/w% gel **2** could not be treated similarly, as it was too rigid. Therefore, the 5 w/w% gel **2** was dissolved in a small amount of acetone, and was poured in a teflon mould that was placed in a petridish containing water. The whole set-up was placed under a beaker to allow slow evaporation of the acetone for 3 days, while leaving the hydrogel saturated with water. A sample (25 mm in diameter) could be cut from the resulting hydrogel film. NMR analysis of the film showed no residual acetone. Drying and weighing of the film showed that it had developed into a 7 w/w% hydrogel, indicating that water had evaporated from the hydrogel. Rheology measurements were performed on Rheometrics ARES equipment. The linear viscoelastic region was determined for these samples at 20 °C, at frequencies of  $\omega = 1$  and 10 rad/s using strains of 1%–100%. Gel **2** gave a constant response up to strains of 30%, while gel **1** and **3** gave constant moduli up to 100% strain. Frequency sweep measurements were performed using a strain of 2% (= 0.02 rad) and applying a sweep from 0.1 rad/s to 100 rad/s. Master curves at 20 °C were constructed from the measurements performed at various temperatures between 20 °C and 40 °C by using the time–temperature superposition principle.

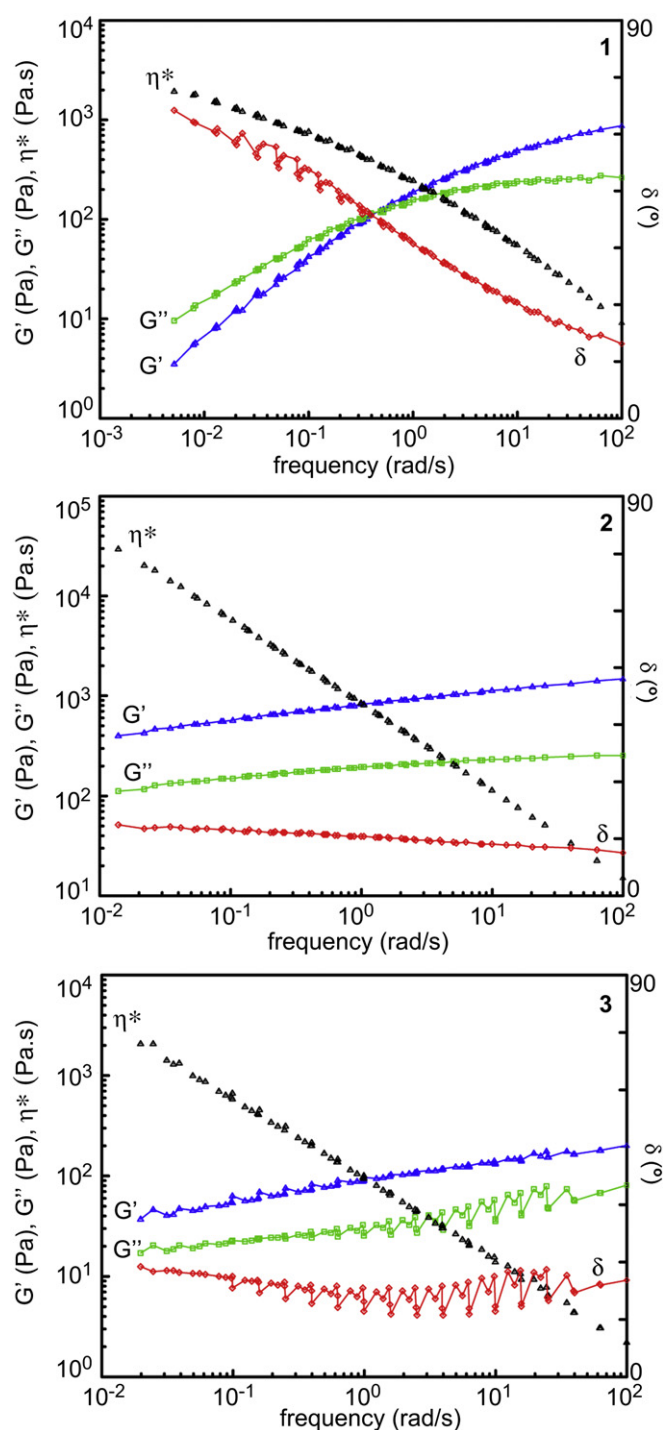


**Fig. 1.** Dynamic mechanical properties. Master curves at 20 °C of the storage modulus  $G'$ , loss modulus  $G''$ , dynamic viscosity  $\eta^*$ , and the phase angle  $\delta$  versus the frequency of gel **1**, **2** and **3**.

### 2.4. In-vitro biocompatibility

The biocompatibility of the dry hydrogelators and hydrogels was tested using human primary tubular epithelial cells (PTEC). PTEC were isolated from renal cortical tissue obtained from patients that underwent unilateral nephrectomy after diagnosis of a urethral or renal tumor. These patients were informed as to the nature of the study and signed a consent form according to Dutch legal requirements. Isolation, culture and characterization were performed as described in the [supplementary information](#) and in the reference [19]. PTEC (passage 2–3) from 3 different donors were seeded in 24-wells plates at a density of  $8.5 \times 10^4$  cells/cm<sup>2</sup> in 0.6 mL medium. The cells were cultured for 3 days (in the case of the 'dry

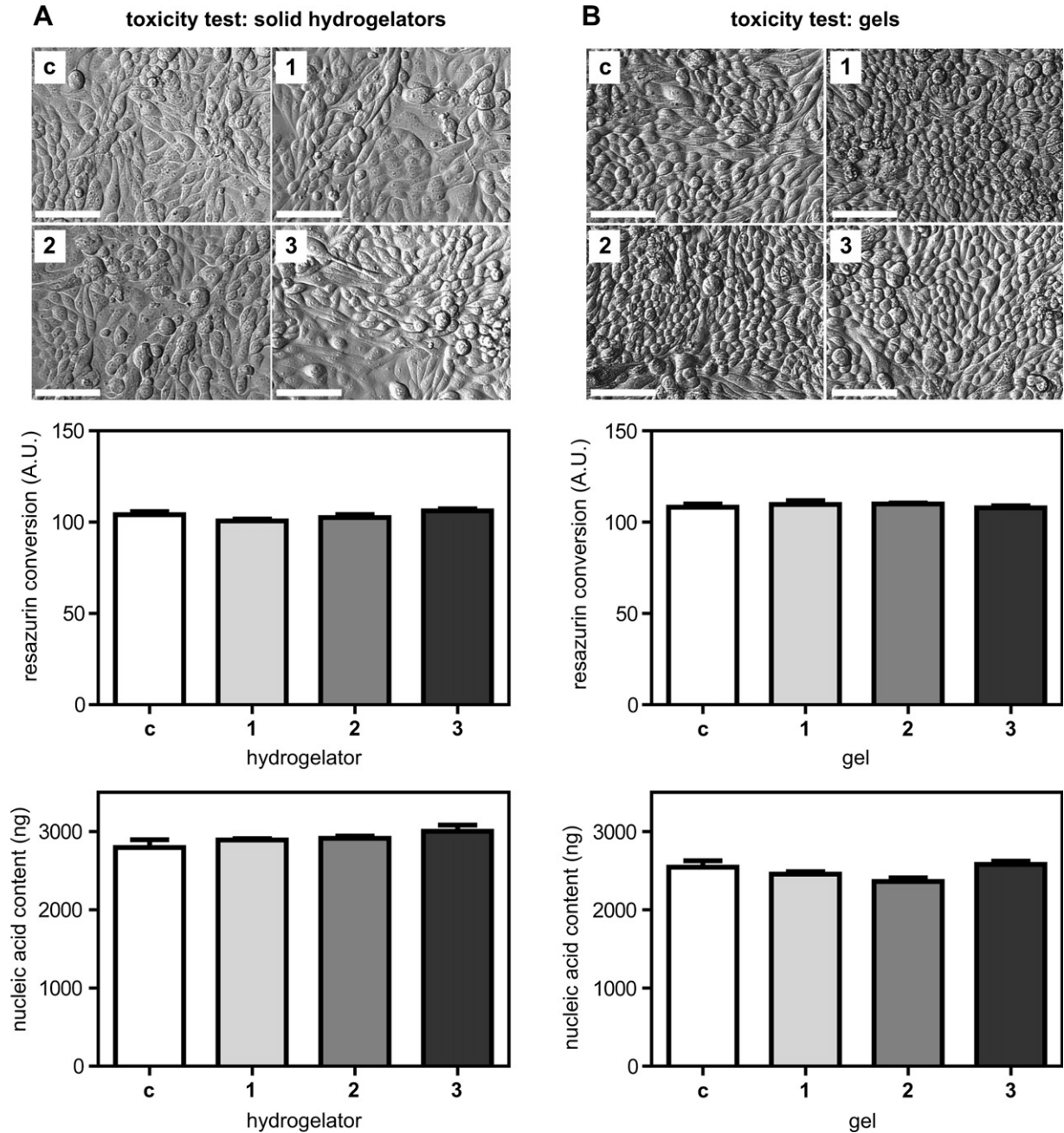


**Fig. 2.** *In-vitro* biocompatibility. The morphology of primary tubular epithelial cells (PTEC) incubated without, i.e. control c, or with 1–3 was visualized by optical microscopy. Scale bars represent 100  $\mu\text{m}$ . Metabolic activity of the PTEC cells was determined by the resazurin assay, and nucleic acid content was determined by the CyQuant assay. These biocompatibility tests were performed on (A) solid hydrogelators and on (B) gels. No statistical differences with the control c were found.

hydrogelator' test) or 4 days (in the case of the 'hydrogel' test) at 37 °C and 5% CO<sub>2</sub>, with intermittent medium changes every 2 days. After 3 days, the cells were washed with PBS and the solid hydrogelator material, sterilized with UV for 1 h, was added in 0.6 mL medium: 50–70 mg/well of hydrogelator 1 or 2 (end concentration of approx. 10 w/w%), 100–150 mg/well of hydrogelator 3 (end concentration of approx. 20 w/w). Alternatively, after 4 days, the cells were washed with PBS and the hydrogels, prepared as described above, were added: 160 mg gel/well in 0.6 mL medium, i.e. end concentration of 1 w/w% 1 or 2, and 2 w/w% 3. The incubations were performed at least in triplicate for every donor-hydrogelator/hydrogel combination. As a reference, cells were cultured in the absence of hydrogelator/hydrogel. The cells were cultured for another 18 h at 37 °C and 5% CO<sub>2</sub>. Optical microscopy pictures of the cells were taken on a Leica DM1L microscope with Leica DC300F camera. Subsequently, the cells were incubated for 2 h at 37 °C in fresh culture medium containing 44  $\mu\text{M}$  resazurin (Sigma Aldrich). Viable cells convert non-fluorescent resazurin into fluorescent resorufin ( $\lambda_{\text{ex}} = 540 \text{ nm}$ ,  $\lambda_{\text{em}} = 590 \text{ nm}$ )

which was measured with a Varioskan plate reader (Thermo Fisher Scientific). After that, the cells were washed twice with PBS and stored at –20 °C. After storage, for at least 18 h the CyQuant Cell Proliferation Assay Kit (Molecular Probes) was used for quantification of nucleic acid content according to the manufacturer's protocol. Fluorescence was measured on the same Varioskan plate reader.

## 2.5. Animals

All animal procedures were approved by the committee for care and use of laboratory animals of the University of Groningen, and performed according to governmental guidelines on animal experimentation. Ten weeks old male Fischer rats (F344, Harlan) with a weight of 230–290 g were used for this study (in total 45 rats). The rats were housed under conventional conditions, in a temperature-controlled and humidity-controlled room with 12 h light/dark cycles. They had access to water and standard rat food *ad libitum*.

## 2.6. Surgical procedures

Rats were anesthetized with a mixture of isoflurane (Abbott) and O<sub>2</sub>. A retro-peritoneal incision was made, and the left kidney was gently lifted through this incision. A subcapsular pocket was generated distal to the ureter, using a blunt needle. The hydrogels **1**, **2** and **3**, 30  $\mu$ L per kidney, were implanted into the subcapsular pocket. The control kidneys received 30  $\mu$ L physiological salt solution (0.9% NaCl solution; B. Braun Melsungen) in the subcapsular pocket. The contralateral kidneys were left untouched. At 3, 7 or 15 days after subcapsular implantation, rats were anesthetized and blood was drawn. The kidneys were perfused *in situ* with PBS, after which they were excised. The kidneys were cut into halves along the sagittal plane. One part was fixed in zinc fixative for 18 h (0.1 M Tris-buffer, 3.2 mM calcium acetate, 23 mM zinc acetate, 37 mM zinc chloride, pH 6.5–7; Merck) and embedded in paraffin. The other part was snap-frozen in liquid N<sub>2</sub> and stored at –80 °C.

## 2.7. Kidney function

The concentration of plasma creatinine in the blood samples was determined using the enzymatic colorimetric CREA plus assay (Roche) [20].

## 2.8. Histological examination

All histological stainings were performed on 5  $\mu$ m zinc-fixed paraffin-embedded sections, which were deparaffinised before use, or on 5  $\mu$ m cryo-sections fixed in acetone in the case of the R73-staining. All stainings were performed at room temperature. Standard washing steps were performed between incubations. After staining, the sections were mounted in permount (Fisher Scientific). Renal morphology was evaluated by periodic acid-Schiff (PAS) staining (15 min 1% periodic acid, 30 min Schiff's reagent (Merck), 5 min hematoxylin 37 °C, 10 s 70% ethanol with 1% hydrochloric acid). For immunohistochemistry, antigen-retrieval was performed on deparaffinised sections, either by incubation in 0.1 M Tris-buffer, pH 9.0 at 80 °C for 18 h (for the ED1 and  $\alpha$ SMA stainings), or by incubation in 0.1% protease (Sigma) for 10 min (for the collagen IV and collagen III stainings). Aspecific staining was blocked with the appropriate 2% animal serum or with 2% bovine serum albumin for 30 min. Endogenous peroxidase was blocked with 0.5–1% hydrogen peroxide (Merck) for 30 min, or with 0.5% phenylhydrazine (Fluka) for 30 min in the case of the collagen IV staining. Endogenous biotin was blocked with a biotin blocking kit (Dako). The sections were incubated with the following primary antibodies for 1 h, and subsequently with the appropriate secondary antibodies for 30 min: mouse anti-rat CD68 (1:200; anti-ED1; Serotec) with secondary antibody rabbit-anti-mouse-peroxidase (1:100; Dako); goat anti-collagen IV (1:150; Southern Biotechnology Associates) with secondary antibody rabbit-anti-goat-peroxidase (1:100; Dako); mouse  $\alpha$ -smooth muscle actin (1:200; Dako) with secondary antibody

rabbit-anti-mouse-peroxidase (1:100; Dako) and additional swine-anti-rabbit-peroxidase (1:100; Dako) for 30 min; rabbit anti-rat collagen III (1:100; Serotec) with secondary antibody goat-anti-rabbit-peroxidase (1:100; Dako) and additional rabbit-anti-goat-peroxidase (1:100; Dako) for 30 min. Colour development was performed using 3,3'-diaminobenzidine tetrachloride (brown; Sigma). If necessary, sections were counterstained with haematoxylin (blue; Merck).

## 2.9. Quantifications

The tissue area studied was in the order of the red box as shown in Fig. 3. The thickness of the fibrous capsule formed around the hydrogel implant during the tissue reaction was measured microscopically at the site of implantation in at least three areas at 200 times magnification using computerized morphometry with Leica QWin 2.8 software. The amount of macrophages in the cortex and the capsule at the site of implantation was determined on tissue sections stained for ED1. Scores in arbitrary units (A.U.) between 0 and 10 were given, where 0 means not present and 10 signifies abundantly available in the tissue section. Staining of  $\alpha$ SMA and of collagen III was measured using computerized morphometry on a Leica DMLB microscope with Leica DC300 camera and Leica QWin 2.8 software. Both the amount of positive staining in the capsule and in the kidney cortex adjacent to the capsule, were measured. The percentage of positive staining of the total area was quantified in at least 5 areas at 200 times magnification. Vascular expression of  $\alpha$ SMA, and vascular and glomerular expression of collagen III were excluded from the measurements.

## 2.10. Statistical analysis

Differences in data were evaluated with the Kruskal–Wallis test followed by Dunn's post-hoc multiple comparison analysis (for the *in-vitro* biocompatibility tests, and kidney function measurements), or using one-way ANOVA followed by post-hoc Newman–Keuls multiple comparison test for data with Gaussian distribution (for the morphometry data). In all cases a 95% confidence interval was used. All data is expressed as mean  $\pm$  standard error of mean. Probabilities of  $P < 0.05$  were considered to be statistically significant;  $P < 0.05$  is depicted as \*,  $P < 0.01$  is shown as \*\*,  $P < 0.001$  is indicated as \*\*\*.

## 3. Results

### 3.1. Synthesis

The three hydrogelators **1–3** were synthesized as described in the supplementary information (Scheme 1A and Supp. Info). In short, telechelic hydroxy-terminated prepolymers PEG3000 **a**,

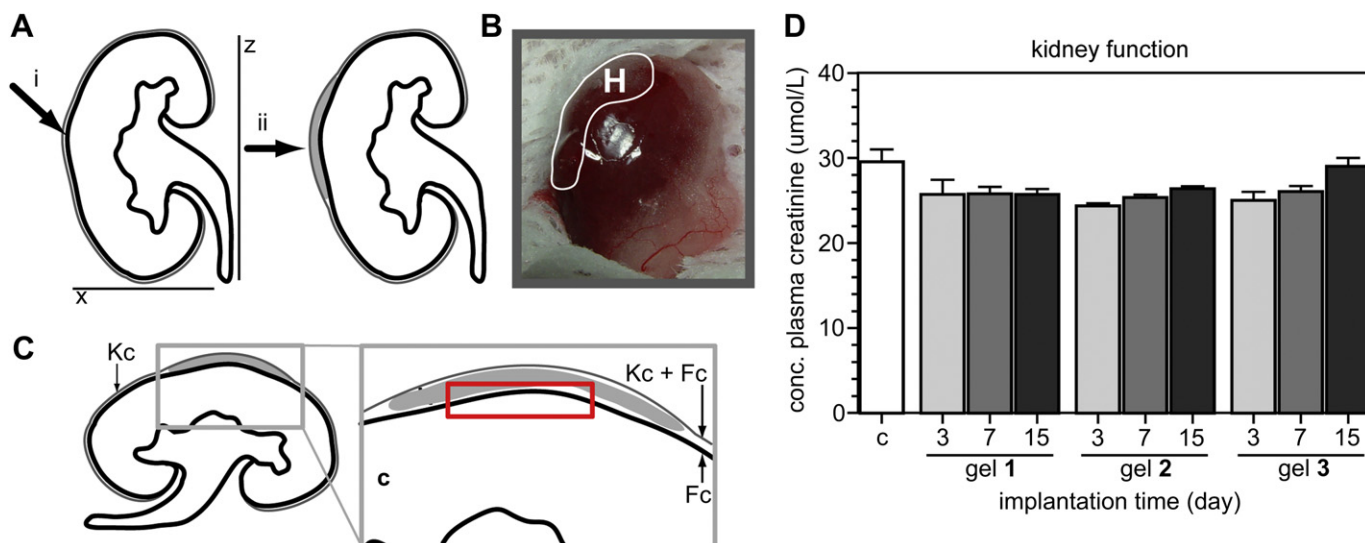
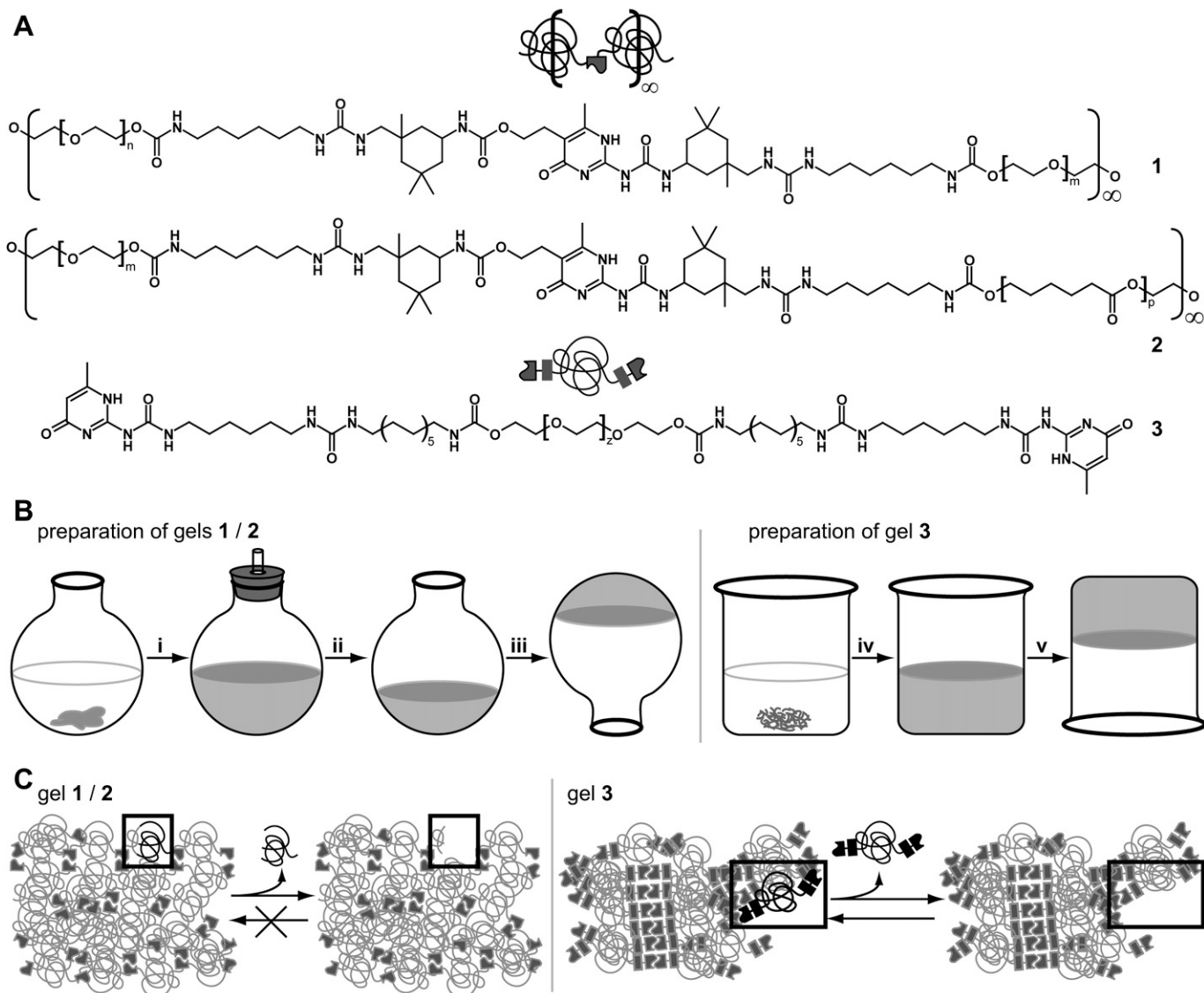


**Fig. 3.** Renal subcapsular implantation procedure and kidney function. (A) Schematic representation of a kidney sliced in the sagittal plane. The average dimensions of a normal rat kidney are depicted by: x is approx. 1 cm, and z is approx. 1.5 cm. The left kidney was gently lifted through a retroperitoneal, dorsal incision. Then, i. the kidney capsule was loosened from the kidney to introduce a small pocket in which ii. 30  $\mu$ L of the gels was implanted. 30  $\mu$ L of saline was introduced in the control kidney c. (B) An example of a gel implanted under the kidney capsule. (C) A schematic representation shows the area at the site of gel implantation, the kidney cortex and the kidney capsule. In time a fibrous capsule is formed around the hydrogel. A combination of the kidney capsule and the fibrous capsule is depicted with Kc + Fc. The area analyzed for histological examination, i.e. arbitrary scoring and morphometry, is shown depicted with a red box. (D) Blood plasma creatinine concentration was determined 3, 7 or 15 days after implantation of the gels. No statistical differences with control animals, which were not operated and did not receive a gel, were found. C = cortex, c = control animals, Fc = fibrous capsule, H = (hydro)gel, Kc = kidney capsule. (For interpretation of the references to colour in this figure legend, the reader is referred to the web version of this article.)





**Scheme 1.** Chemical structures of the supramolecular ureido-pyrimidinone (UPy) modified hydrogelators, gel preparation, and proposed degradation behaviour. (A) Two chain-extended UPy-modified hydrogelators, **1** and **2**, were used; **1** based on either PEG with  $M_n = 3000$  and  $M_n = 6000$  g/mol in a ratio of 1:1 w/w%, and **2** based on both PEG with  $M_n = 6000$  g/mol and PCL with  $M_n = 1250$  g/mol with a ratio of 9:1 w/w%. One end-functionalized UPy-hydrogelator **3** was investigated, based on PEG with  $M_n = 20,000$  g/mol. (B) Gelation procedure of UPy-hydrogelators **1-3**: i. Prepolymers **1** or **2** were dissolved in a mixture of 1:1 THF:0.9% NaCl aqueous solution by stirring at 21 °C ii. THF is removed *in vacuo* to obtain 5 w/w% gels. iii. After removal of THF the gels were formed. iv. Prepolymer **3** was dissolved in water by stirring at 60 °C v. The solution was cooled to 21 °C to gelate, and to obtain a 10 w/w% gel. (C) Schematic representation of the proposed degradation behaviour: conventional hydrolysis must occur for gels **1** and **2** to degrade, and gel **3** is able to erode via a supramolecular degradation mechanism.

PEG6000 **b**, PCL1250 **c**, and PEG20000 **d** were activated with 1,1-carbonyldiimidazole (CDI). The resulting CDI-activated prepolymers were reacted with 1,6-hexyldiamine for **4a–c**, or with 1,12-dodecyldiamine in the case of **4d**, yielding diamine-terminated polymers **5a–d**. Reaction of diamine-terminated **5a** and **5b** in 1:1 w/w% ratio with 1 equivalent IPDI-UPy-IPDI synthon [11] yielded **1** as a white, semi-crystalline, elastic, tough material. This chain-extended hydrogelator **1** contained PEG3000, PEG6000 and a high number of UPy-moieties per polymer chain. Chain-extended hydrogelator **2** was synthesized in a similar way from **5b**, **5c** and IPDI-UPy-IPDI, which resulted in a white, semi-crystalline, elastic, tough UPy-co-polymeric material of PEG6000 and PCL1250 in 9:1 w/w% ratio. Via reaction of the diamine-terminated PEG20000 **5d**, with the UPy-hexyl-isocyanate synthon [11], bifunctional hydrogelator **3** was obtained as a white powder.

### 3.2. Gelation procedures and degradation behaviour

The gelation procedure for the chain-extended and the bifunctional hydrogelators differed. Whereas organic solvent was required to form the chain-extended hydrogels, for gelation of the bifunctional hydrogelator application of only an aqueous solution was adequate (Scheme 1B). The chain-extended hydrogelators were dissolved in THF, after which a physiological salt solution was added. THF was removed under reduced pressure, and soft and elastic 5 w/w% hydrogels were formed. Relatively, hydrogel **2** was more rigid and shape-persistent than hydrogel **1**. Hydrogelator **3** was dissolved in a physiological salt solution at 60 °C, and subsequently allowed to set at 21 °C yielding a soft hydrogel. Short incubation, i.e. for 18 h, of 0.05–0.2 g of the hydrogels **1–3** at 37 °C in 1 mL water, buffer or cell culture medium showed that hydrogel **1** and **2** did not undergo visible changes, while gel **3** was completely

dissolved. Apparently, the chain-extended hydrogelators cannot be molecularly dissolved in water because of the higher molecular weight of these macromolecules and the multiple UPy-units per chain. Therefore, an organic solvent is needed which provides an environment in which these hydrogelators can (partially) dissolve. The gelation process takes place after addition of water and removal of the organic solvent. In contrast, the bifunctional hydrogelator dissolves in water at elevated temperatures, and gels after cooling to room temperature.

According to these findings we propose that the chain-extended hydrogels can only degrade by hydrolysis, and not by dissolution of entire polymer chains (Scheme 1C). The bifunctional hydrogelator gels *in situ* in an aqueous environment, indicating that a totally different process occurs. It is proposed that in order to form a hydrogel, the UPy-dimers of **3** have to form fibers by  $\pi$ - $\pi$  interactions, additional hydrogen bonding between the urea-groups, and accessory hydrophobic interactions of the dodecyl spacers. The bifunctional hydrogels will erode by dissolution of single chains or small polymeric aggregates, i.e. via supramolecular degradation (Fig. 2B). It is expected that similar dissolution behaviour of the hydrogels is manifested *in vivo* after subcapsular implantation in the kidney; experimental details will be discussed below. The exact mechanism of hydrogel formation and erosion of similar bifunctional UPy-hydrogelators *in vitro* has been investigated extensively in another study [18].

### 3.3. Rheological properties

The mechanical properties of the hydrogels were investigated using rheology (Fig. 1). Hydrogel **1** shows pronounced viscoelastic behaviour as the moduli and the viscosity are strongly frequency-dependent. At lower frequencies the material has fluid-like properties;  $G'' > G'$ , i.e. the flow domain. At higher frequencies elastic behaviour is observed;  $G' > G''$ , i.e. the rubber plateau. Hydrogel **1** is very elastic but can flow in time showing 'creep' behaviour. This implies that upon sudden stresses, i.e. shorter time scales, the material can elastically be deformed and reformed, while at longer time scales it can adjust its shape to minimize persistent surrounding stresses. The other two hydrogels, **2** and **3**, display a rubber plateau over the whole frequency domain measured. Therefore, these materials are more shape persistent. Hydrogel **2** is more rigid than hydrogel **3** because of its higher storage modulus  $G'$  over the whole frequency domain. Hydrogel **2** has a  $G'$  of approximately 1000 Pa, whereas **3** shows a  $G'$  of approximately 100 Pa.

### 3.4. In-vitro biocompatibility

Prior to *in-vivo* subcapsular implantation, the *in-vitro* biocompatibility was assessed as a predictor of *in-vivo* behaviour. *In-vitro* biocompatibility was investigated using human primary tubular epithelial cells (PTEC) [19] as a model for the renal setting (Fig. 2). The biocompatibility of materials **1–3** was determined by culture of PTEC in the presence of materials **1–3**, as dry hydrogelator or hydrogel. Biocompatibility was assessed by morphological examination of the cells, metabolic activity (determined in the resazurin assay) and nucleic acid content (determined by CyQuant assay) (Fig. 2). In all three assays, no differences were found between cells cultured in the presence of materials and cells cultured in pristine culture medium (Fig. 2). In addition, the materials were tested for the presence of bacterial endotoxin, which is known to cause inflammation *in vivo*. The UPy-modified hydrogelators contained approximately 14–23 times less endotoxin than the value permitted by the FDA 0.5 EU/mL (0.036 EU/mL for 5 w/w% **1**, 0.022 EU/mL for 5 w/w% **2**, 0.026 EU/mL for 10 w/w% **3** in water). These results show that **1–3** are not toxic and are safe for *in-vivo* use.

### 3.5. Renal implantation and explantation

In the clinical setting, the introduction of a drug delivery system under the renal capsule should preferably be non or minimally invasive. Hydrogels **1–3** were implanted under the capsule of rat kidneys by injection, a process that required the generation of a subcapsular pocket by gently detaching the capsule from the renal cortex (Fig. 3A and B). To assess the possible effect of subcapsular hydrogel implantation on renal function, plasma creatinine levels were measured at day 3, 7 and 15 after implantation (Fig. 3D). No differences in creatinine levels were found between control animals (that received a subcapsular saline solution) and experimental groups (that received subcapsular hydrogel implants), indicating no deterioration of renal function. The area below the site of implantation was examined histologically via arbitrary scoring and morphometry (the area is depicted with a red box in Fig. 3C). Upon explantation of the kidneys, hydrogel **1** and **2** were macroscopically detectable at all time points, after 3, 7 and 15 days, whereas hydrogel **3** was not visible at any time point. Enhanced vascularisation around both hydrogel **1** and **2** was detected macroscopically at day 15.

### 3.6. Cortical tissue response

It is conceivable that renal subcapsular implantation of a drug delivery carrier can trigger cortical modifications due to the implantation procedure and/or the tissue reaction to the materials implanted. Ideally, the implantation should not affect cortical integrity, or cause severe adverse reactions such as inflammation or fibrosis. After implantation of hydrogels **1–3** or saline injection, slight cortical modification immediately below the site of implantation was observed, but not at sites distal from the implantation site. Therefore, we selected this site to study the cortical tissue response to hydrogel implantation.

The inflammatory reaction was investigated by macrophage ( $M\phi$ ) staining using ED-1 as a marker (Fig. 4A,B). No  $M\phi$  were present in the tubulointerstitial space of contralateral kidneys at any time point studied. In kidneys injected with saline, a mild tubulointerstitial infiltration was observed at all time points, with the exception of day 7, where a higher infiltration was possibly caused by the implantation procedure.  $M\phi$  infiltration in kidneys implanted with **1** was stable over time and comparably mild as in saline-injected kidneys. At day 3, after implantation of **2**  $M\phi$  infiltration was comparable to kidneys receiving saline or **1**, but increased at day 7, and slightly decreased at day 15. A similar response was observed after implantation of **3**. Overall, hydrogel **1** elicited the mildest response of the three hydrogels. However, the strong local restriction of macrophages in the interstitial space immediately below the implantation site and their transient presence indicated that all three gels displayed a virtually negligible cortical inflammatory response.

To determine whether hydrogel implantation elicited the formation of interstitial myofibroblasts, kidneys were stained for  $\alpha$ -smooth muscle actin ( $\alpha$ SMA) (Fig. 5A,B). No interstitial myofibroblasts were observed in contralateral kidneys at any time point. In kidneys injected with saline, interstitial myofibroblasts accounted for approximately 2% of the cortical area at all time points. Hydrogel **1** elicited virtually no interstitial myofibroblast formation at early time points, whereas at day 15 myofibroblast numbers slightly exceeded those found in saline control kidneys. Hydrogel **2** evoked transient interstitial myofibroblast formation that peaked 7 days after implantation but was comparable to control levels at day 3 and day 15. In kidneys implanted with hydrogel **3**, myofibroblast numbers did not exceed control values, although spots of  $\alpha$ SMA staining were detected occasionally. Overall, the implantation of all



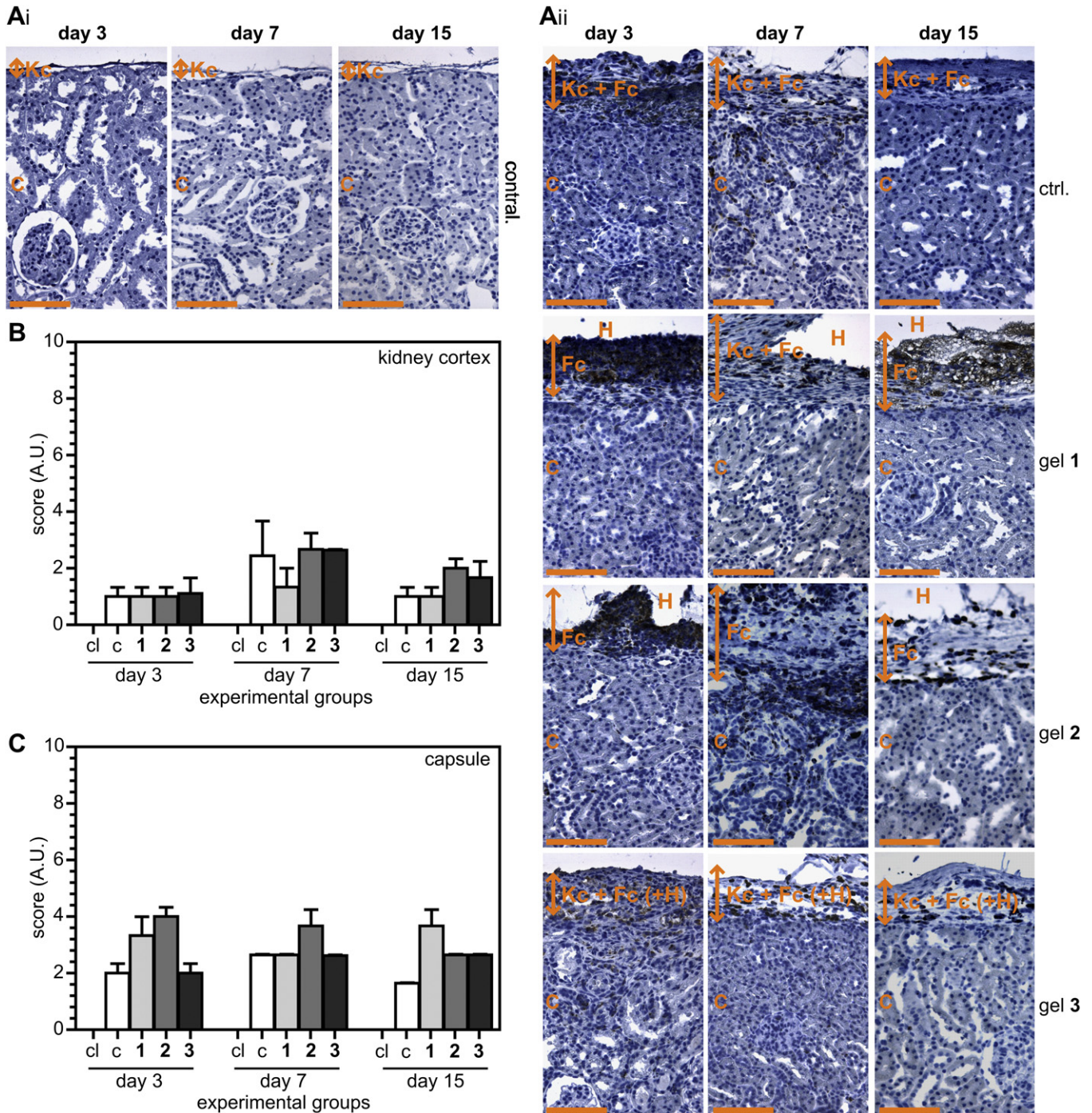


**Fig. 4.** Macrophage infiltration in the cortex and capsule under the implantation site. (Ai and Aii) Tissue slices were stained for the macrophage marker ED1 3, 7 and 15 days after implantation. The double arrows depict the kidney capsule in the contralateral kidneys; the thickened, fibrous kidney capsule, i.e. Kc + Fc, in the control kidneys; the fibrous capsule for the experimental kidneys with gels 1 and 2; and the fibrous kidney capsule with possible gel remnants, i.e. Kc + Fc (+H) for the experimental kidneys with gel 3. All scale bars represent 100  $\mu$ m. Contral. = contralateral kidney, ctrl. = control kidneys, C = cortex, Fc = fibrous capsule, H = (hydro)gel, Kc = kidney capsule. Arbitrary scoring of amount of macrophages in (B) the cortex and (C) the capsule. (For interpretation of the references to colour in this figure, the reader is referred to the web version of this article.)

three hydrogels was associated with a relatively negligible and locally restricted presence of myofibroblasts in the renal cortex, with exception of hydrogel 2 in which a transient cortical accumulation of myofibroblasts 7 days after implantation was detected.

Myofibroblasts are key players in fibrosis by producing extracellular matrix (ECM) proteins. One of these ECM proteins is collagen III, a component of tubular basal membranes that is deposited in the renal interstitium during fibrosis. To investigate

whether subcapsular hydrogel implantation elicited collagen III deposition in the kidney, collagen III staining was quantified by morphometry (Fig. 6A,B). Comparable amounts of collagen III deposition were found in contralateral and saline control kidneys at all time points. The implantation of hydrogels 1 and 3 was associated with cortical collagen III deposition similar to the control kidneys, irrespective of the time point. Hydrogel 2 elicited a transiently elevated collagen III deposition at day 7, whereas at day 3 and



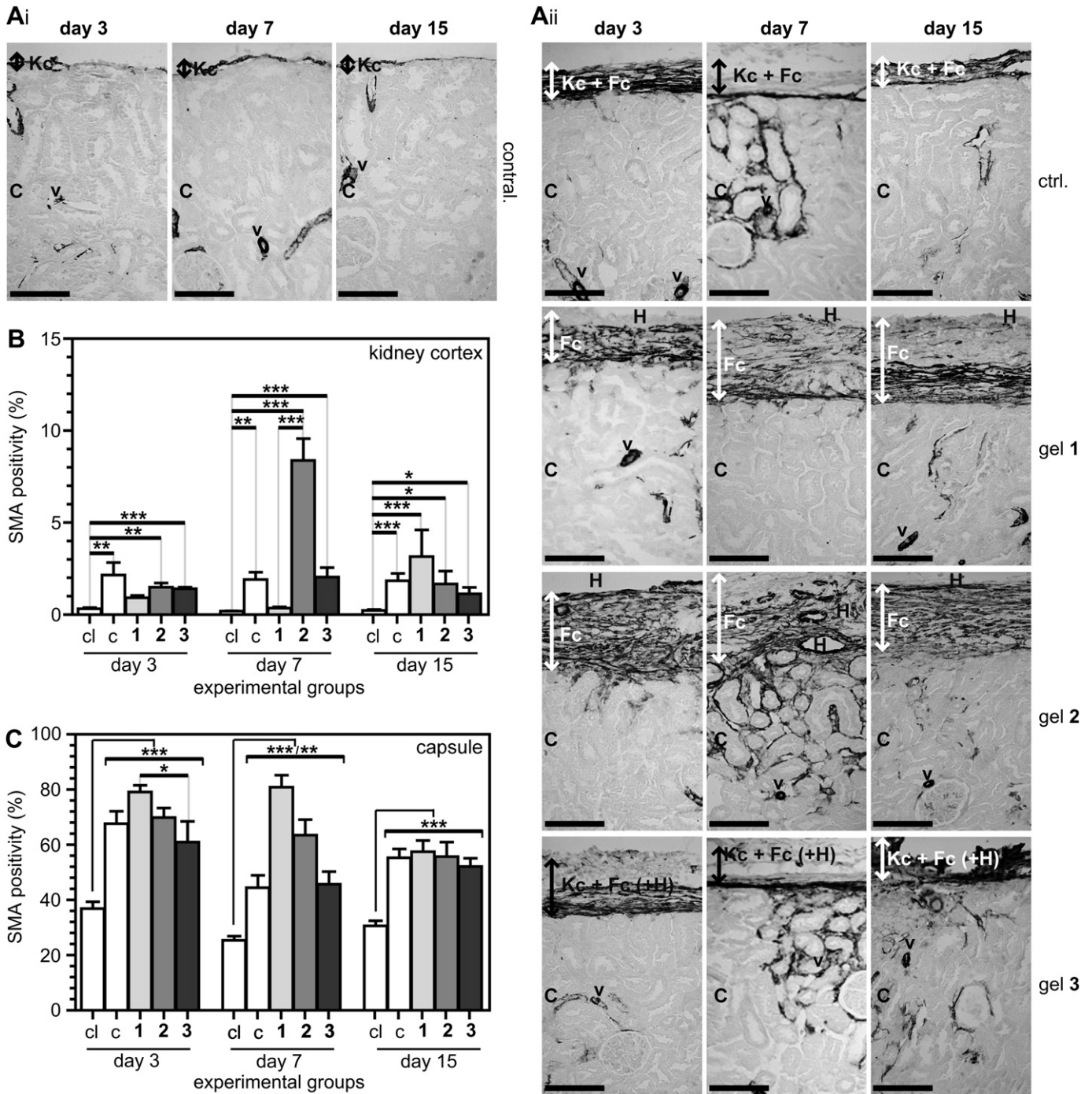


**Fig. 5.** Detection of myofibroblasts in the kidney cortex and the capsule under the implantation site. (Ai and Aii) Myofibroblasts were stained for  $\alpha$ -smooth muscle actin after 3, 7 and 15 days of implantation. The double arrows depict the kidney capsule in the contralateral kidneys; the fibrous, kidney capsule, i.e. Kc + Fc, in the control kidneys; the fibrous capsule for the experimental kidneys with gels 1 and 2; and the fibrous kidney capsule with possible gel remnants, i.e. Kc + Fc (+H), for the experimental kidneys with gel 3. All scale bars represent 100  $\mu$ m. Contral. = contralateral kidney, ctrl. = control kidneys, C = cortex, Fc = fibrous capsule, H = (hydro)gel, Kc = kidney capsule, v = blood vessels. The amount of myofibroblasts was quantified by morphometry in (B) the cortex and (C) the capsule, as depicted in Fig. 3.

day 15 no differences were observed as compared to the controls. Interestingly, this increase in collagen III paralleled the increase in  $\alpha$ SMA staining observed at day 7 after implantation of gel 2.

The low  $\alpha$ SMA-positivity and low M $\phi$  infiltration after 15 days, together with the lack of differences with respect to the amount of collagen III between the kidneys with hydrogels 1 and 3 and contralateral kidneys, might be explained by the fact that enhanced ECM deposition, and thus deposition of collagen III, is only up-regulated after more extensive damage or sustained inflammation.

This indicates that subcapsular implantation of hydrogels 1 and 3 does hardly damage the renal cortex. The tissue response for hydrogel 2 was detected to be slightly less mild.

### 3.7. Subcapsular foreign body reaction

The introduction of a biomaterial in the body typically elicits a foreign body reaction (FBR), which aims at encapsulation of the biomaterial for the protection of the surrounding tissue and at its



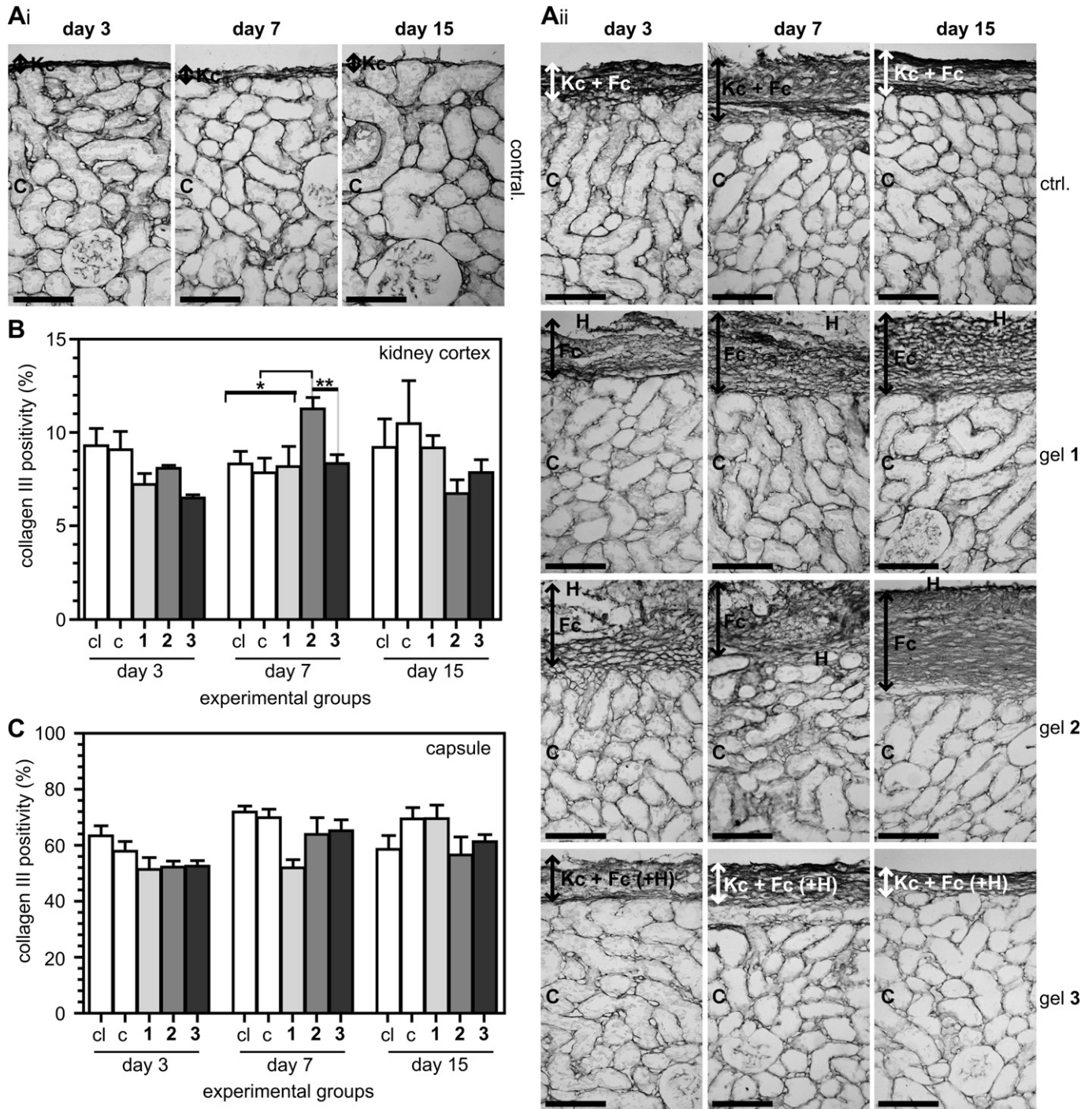


**Fig. 6.** The presence of interstitial collagen III in the capsule and cortex under the implantation site. (Ai and Aii) Tissue slices were stained for collagen III after 3, 7 and 15 days of implantation. The double arrows depict the kidney capsule in the contralateral kidneys; the fibrous kidney capsule, i.e. Kc + Fc, in the control kidneys; the fibrous capsule for the experimental kidneys with gels 1 and 2; and the fibrous kidney capsule with possible gel remnants, Kc + Fc (+H), for the experimental kidneys with gel 3. All scale bars represent 100  $\mu$ m. Contral. = contralateral kidney, ctrl. = control kidneys, C = cortex, Fc = fibrous capsule, H = (hydro)gel, Kc = kidney capsule. The amount of collagen III was quantified by morphometry in (B) the cortex and (C) the capsule, as depicted in Fig. 3.

removal by macrophage-mediated phagocytosis. In our present subcapsular implantation model, saline-treated control kidneys were used to distinguish between capsular alterations caused by the pocket surgery and FBR-related phenomena. The generation of a subcapsular pocket and subsequent administration of saline in the pocket induced significant, capsule thickening after 3 and 7 days, although the process was reversed to a large extent by day 15

(Supp. Info). Upon implantation of hydrogels 1 and 2, thickening of the kidney capsule was observed as well, while a fibrous, FBR-related encapsulation was observed at the cortical side of the implants. This latter phenomenon was not observed after implantation of hydrogel 3, possibly due to its rapid degradation. Quantification of kidney capsule thickness revealed time and material-dependent differences. After implantation of hydrogel 1, the

capsule thickness resembled that of the saline receiving control kidneys, but increased gradually until day 15. Implantation of hydrogel **2** led to significantly more capsule thickening than saline control injection. However, capsule thickness remained relatively stable over time. After implantation of hydrogel **3**, the thickness of the capsule equalled that of saline controls and increased transiently by day 7 (Supp. Info).

Collagen IV is both present in the basement membranes of blood vessels, tubuli and glomeruli, consequently it is difficult to distinguish between these structures. Therefore, collagen IV staining was used to particularly investigate vascularisation in the capsule (Supp. Info). Whereas the distinctions between the groups were less clear after 3 days, the differences became more apparent after 7 and 15 days. The amount of vascularisation became higher for kidneys containing hydrogels **1** or **2**, and progressed until day 15. This was already detected macroscopically during explantation of kidneys with hydrogels **1** and **2** after 15 days. In the case of the control kidneys and the kidneys with hydrogel **3**, the amount of blood vessels seemed to be reduced after 15 days.

As mentioned previously, the infiltration of  $M\phi$  is a hallmark of the FBR. In saline-treated kidneys,  $M\phi$  were present in the thickened kidney capsule and at the interface between the loosened kidney capsule and the cortex, indicating that the surgical procedure elicited a mild tissue response. Upon implantation of hydrogels **1–3**,  $M\phi$  infiltration was detected in the thickened kidney capsules at all time points, suggesting that the subcapsular vascular network might be the entry route of these cells at the implantation site. For each hydrogel, the amount of FBR-related  $M\phi$  remained relatively stable in time (Fig. 4C). Occasionally, giant cells and foam cells were detected in the FBR associated with hydrogels **1** and **2** (Supp. Info).

Surgical and FBR-related renal capsule thickening was also investigated by detection and quantification of  $\alpha$ SMA expressing myofibroblasts (Fig. 5C). In contralateral kidneys, myofibroblasts were detected as constituents of the renal capsule. In saline-treated kidneys, the amount of  $\alpha$ SMA staining was higher at all time points studied, indicating that capsular thickening after generation of the subcapsular pocket was mediated by myofibroblasts. In general,  $\alpha$ SMA-positivity in the kidney capsule was comparable to that in control kidneys after implantation of all three hydrogels at the beginning (day 3) and at the end (day 15) of the observation period (Fig. 5C). Material-related differences in capsular  $\alpha$ SMA-positivity were observed at day 7, where gel **2** elicited the highest myofibroblasts formation and implantation of gel **3** resulted in similar  $\alpha$ SMA-positivity as saline injection.

#### 4. Discussion

Irrespective of the nature of the damage, kidney injury is invariably associated with inflammation. Improper resolution or chronic persistence of inflammation sets the stage for fibrosis, which has been identified as the common pathway to kidney failure. Inflammation and fibrosis of the tubulointerstitial space cannot be effectively addressed by systemic drug administration. Moreover, systemic drug administration is associated with the loss of the therapeutic compounds to irrelevant sites in the body and with undesired side effects, as is exemplified by immune-suppressive treatment after kidney transplantation. Therefore, various areas of kidney therapy would profit from a therapeutic device that allows local drug delivery into the renal interstitium in order to modulate tubulointerstitial inflammation and fibrosis, to promote renal repair, and in this way to prevent progression towards chronic renal damage and failure.

Here we present the synthesis and *in-vivo* kidney compatibility of supramolecular hydrogels designed for intrarenal drug delivery.

Intrarenal drug delivery from a hydrogel carrier implanted under the kidney capsule might be an innovative way to induce kidney tissue regeneration and/or prevent kidney inflammation or fibrosis. In order to investigate the feasibility of this approach it is important to first study the tissue response to these carriers when implanted under the kidney capsule. Subcutaneous implantation studies will not be adequate because it has been shown previously that the tissue response differ between different implantation sites [21].

We designed and synthesised three different supramolecular UPy-modified poly(ethylene glycol) hydrogels for intrarenal implantation. We have chosen to use supramolecular hydrogelators because the directed non-covalent interactions taking care of network formation give the materials dynamic properties complying with intrarenal implantation, i.e. the requirement for distribution and spreading of the material under the kidney capsule. Two chain-extended UPy-polymers, with the UPy-units part of the main chain, and one bifunctional UPy-polymer, in which the two chain ends were modified with UPy-moieties, were synthesized. The differences in properties were immediately clear from the method of formulation of these hydrogelators into hydrogels. Whereas the end-functionalized material could be readily dissolved in water at elevated temperatures, the chain-extended materials required the addition of organic solvent to be dissolved. Gelation took place after cooling down to room temperature (for the bifunctional hydrogelator), or after removal of the organic solvent under reduced pressure (for the chain-extended hydrogelators).

After hydrogel formation the bifunctional hydrogel erodes fast upon addition of water, while the chain-extended hydrogels remained stable in time. Rheology showed that the chain-extended materials form strong, flexible hydrogels, and the bifunctional material forms a weaker, soft hydrogel. The differences between these two classes of hydrogels with respect to their physico-chemical properties were also reflected in the results obtained after subcapsular implantation in kidneys.

The subcapsular application of a drug delivery device should ideally not affect the structure and function of the kidney or evoke a tissue response such as inflammation or fibrosis. This is crucial for implantation in the kidneys since these organs are sensitive to stress. We showed that partial surgical detachment of the kidney capsule in order to generate a pocket for hydrogel implantation leads to capsular thickening, which did not appear to be deleterious to kidney structure or function. Importantly, both the subcapsular FBR and the cortical presence of macrophages and myofibroblasts were highly restricted to the site of implantation, irrespective of hydrogel type, although variations between hydrogels were observed. Differences in tissue response to the two chain-extended hydrogels could be detected; the more elastic hydrogel induced a tissue response which was located at the interface between hydrogel and kidney tissue, while the tougher, more shape-persistent hydrogel additionally induced slight damage to the cortex. It is proposed that the tougher hydrogel cannot easily adjust itself to the pocket created between the renal capsule and the cortex; therefore we reason that this hydrogel exerts more pressure on the cortex thereby inducing more damage. Fifteen days after implantation, the bifunctional hydrogel ultimately showed the lowest tissue response of all three hydrogels tested. After injection it was immediately observed that this hydrogel could fill up the complete pocket by spreading. In this way, the hydrogel was homogeneously distributed and did not exert force on the kidney cortex. The tissue response was similar to the control kidneys in which only the kidney capsule was loosened. The damage to the cortex was minimal, and a fibrous capsule was hardly formed. Additionally, the erosion behaviour of the two classes of hydrogels



*in vivo* was different. The chain-extended UPy-hydrogels did not show a sign of degradation after two weeks. The end-functionalized was resorbed within days, which we address to supramolecular erosion, i.e. complete dissolution of the supramolecular polymer aggregates without chemical cleavage of bonds by hydrolysis. This also explains the minimal tissue response induced by this hydrogel. Furthermore, from our rheological data in combination with the *in vivo* data we derive that kidneys are able to deal with soft hydrogels, or more particularly, (visco)-elastic hydrogels that have  $G'$ -values that are preferably lower than  $10^3$  Pa.

With respect to future clinical applications as kidney drug delivery vehicles, the minimal tissue response to the bifunctional hydrogel and the fast degradation behaviour makes it suitable for short-time boost release of drugs. Moreover, the stability of this hydrogel can be easily adjusted by introduction of additional carbon atoms in the alkyl spacer and/or shortening the length of the PEG chain [18]. The green, organic-solvent free preparation method of the bifunctional hydrogel makes it eminently suitable as (growth factor) protein drug delivery vehicle. Very recently we provided the proof-of-concept that the formulation of the anti-fibrotic growth factor BMP7 is feasible in this hydrogel with preservation of its biological activity [18]. Moreover, local intrarenal delivery of BMP7 clearly inhibited formation of myofibroblasts in the renal cortex after subcapsular administration in the bifunctional hydrogel [18].

We propose that the chain-extended hydrogels can be used for long-term release studies, although incorporation of protein drugs into these chain-extended hydrogels might be a challenge because of the need for organic solvent in the formulation process. On the contrary, the release of organic drugs from the chain-extended hydrogels is very much possible as such drugs can in general withstand harsher formulation conditions. Moreover, the mechanical and solution vs. hydrogel performance of these chain-extended hydrogels can also be easily adjusted by tuning the chain length of the PEG-block and the nature of the alkyl linker. The minimal cortical damage and the mild tissue response to all three hydrogel systems show that these supramolecular hydrogels can be applied as subcapsular vehicles for intrarenal drug delivery. Currently, we are investigating the administration of BMP7 from subcapsularly implanted supramolecular hydrogels after kidney ischemia-reperfusion injury.

## 5. Conclusions

We have successfully synthesized three different supramolecular hydrogelators based on PEG chains and UPy-moieties. Two chain-extended hydrogelators possessing UPy-units in the main chain, and one bifunctional hydrogelator with UPy-groups at the chain end, were produced. A mixture of water and organic solvent was needed to dissolve the chain-extended hydrogelators. Gelation took place after removal of the organic solvent. In contrast, the bifunctional hydrogelator could be dissolved in only water at elevated temperature. Subsequently, the hydrogel was formed after cooling to ambient temperature. The chain-extended polymers both formed strong, elastic hydrogels; one was more flexible, while the other was tougher. The end-functionalized UPy-hydrogelator formed a weaker and softer hydrogel. Implantation of these three different hydrogels under the renal capsule resulted in mild tissue responses. The reaction to the more flexible chain-extended hydrogel was located at the interface between renal tissue and hydrogel, whereas the tougher chain-extended hydrogel also induced slight damage to the renal cortex. The bifunctional hydrogel showed a minimal tissue response which was comparable to the control kidneys in which only the renal capsule was loosened. The chain-extended UPy-hydrogels did not degrade after two

weeks, while the bifunctional hydrogel was resorbed within days, which is proposed to occur by dissolution of entire polymer aggregates. The properties and *in vivo* behaviour of the bifunctional hydrogel makes it an attractive intrarenal drug carrier for short-term protein delivery, while the properties of one of the chain-extended hydrogels makes this hydrogel possibly suitable for long term intrarenal delivery of organic drugs.

## Acknowledgements

We acknowledge Jan van der Wijk and Frank Smedts for supplying the kidney tissues, Jasper Koerts for cutting the tissue slices, Heleen Rienstra and the clinical chemistry laboratory for performing the creatinine measurements, and Martine Broekema, Marco Harmsen, Jasper Boomker and Travis Baughman for useful discussions. This work is supported by SupraPolix, and the Council for Chemical Sciences of the Netherlands Organization for Scientific Research (CW-NWO).

## Appendix A. Supplementary data

Supplementary data related to this article can be found online at doi:10.1016/j.biomaterials.2012.03.052.

## References

- [1] Dolman MEM, Harmsen S, Storm G, Hennink WE, Kok RJ. Drug targeting to the kidney: advances in the active targeting of therapeutics to proximal tubular cells. *Adv Drug Deliv Rev* 2010;62(14):1344–57.
- [2] Yu L, Ding JD. Injectable hydrogels as unique biomedical materials. *Chem Soc Rev* 2008;37(8):1473–81.
- [3] Peppas NA, Hilt JZ, Khademhosseini A, Langer R. Hydrogels in biology and medicine: from molecular principles to bionanotechnology. *Adv Mater* 2006;18(11):1345–60.
- [4] Lynn AD, Blakney AK, Kyriakides TR, Bryant SJ. Temporal progression of the host response to implanted poly(ethylene glycol)-based hydrogels. *J Biomed Mater Res Part A* 2011;96A(4):621–31.
- [5] Bolgen N, Vargel I, Korkusuz P, Guzel E, Plieva F, Galaev I, et al. Tissue responses to novel tissue engineering biodegradable cryogel scaffolds: an animal model. *J Biomed Mater Res Part A* 2009;91(1):60–8.
- [6] Azab AK, Doviner V, Orkin B, Kleinstem J, Srebnik M, Nissan A, et al. Biocompatibility evaluation of crosslinked chitosan hydrogels after subcutaneous and intraperitoneal implantation in the rat. *J Biomed Mater Res Part A* 2007;83A(2):414–22.
- [7] Merani S, Toso C, Emamullee J, Shapiro AMJ. Optimal implantation site for pancreatic islet transplantation. *Br J Surg* 2008;95(12):1449–61.
- [8] Cole DR, Waterfall M, McIntyre M, Baird JC. Transplantation of microcapsules (a potential bioartificial organ) – biocompatibility and host-reaction. *J Mater Sci – Mater Med* 1993;4(5):437–42.
- [9] Lanza RP, Kuhlreiber WM, Ecker D, Staruk JE, Chick WL. Xenotransplantation of porcine and bovine islets without immunosuppression using uncoated alginate microspheres. *Transplantation* 1995;59(10):1377–84.
- [10] Sijbesma RP, Beijer FH, Brunsvelde L, Folmer BJB, Hirschberg JHKK, Lange RFM, et al. Reversible polymers formed from self-complementary monomers using quadruple hydrogen bonding. *Science* 1997;278(5343):1601–4.
- [11] Dankers PYW, van Leeuwen ENM, van Gemert GML, Spiering AJH, Harmsen MC, Brouwer LA, et al. Chemical and biological properties of supramolecular polymer systems based on oligocaprolactones. *Biomaterials* 2006;27(32):5490–501.
- [12] Dankers PYW, Zhang Z, Wisse E, Grijpma DW, Sijbesma RP, Feijen J, et al. Oligo(trimethylene carbonate)-based supramolecular biomaterials. *Macromolecules* 2006;39(25):8763–71.
- [13] Söntjens SHM, Renken RAE, van Gemert GML, Engels TAP, Bosman AW, Janssen HM, et al. Thermoplastic elastomers based on strong and well-defined hydrogen-bonding interactions. *Macromolecules* 2008;41(15):5703–8.
- [14] Dankers PYW, Harmsen MC, Brouwer LA, van Luyn MJA, Meijer EW. A modular and supramolecular approach to bioactive scaffolds for tissue engineering. *Nat Mater* 2005;4(7):568–74.
- [15] Wisse E, Spiering AJH, Dankers PYW, Mezari B, Magusin P, Meijer EW. Multicomponent supramolecular thermoplastic elastomer with peptide-modified nanofibers. *J Polym Sci Part A Polym Chem* 2011;49(8):1764–71.
- [16] Luttkhuizen DT, Dankers PYW, Harmsen MC, van Luyn MJA. Material dependent differences in inflammatory gene expression by giant cells during the foreign body reaction. *J Biomed Mater Res Part A* 2007;83A(3):879–86.
- [17] Klerk LA, Dankers PYW, Popa ER, Bosman AW, Sanders ME, Reedquist KA, et al. TOF-secondary ion mass spectrometry imaging of polymeric scaffolds



- with surrounding tissue after in vivo implantation. *Analyt Chem* 2010;82(11):4337–43.
- [18] Dankers PYW, Hermans TM, Baughman TW, Kamikawa Y, Kieleyka RE, Bastings MC, et al. Hierarchical formation of supramolecular transient networks in water: a modular injectable delivery system. *Adv Mater*, in press.
- [19] Dankers PYW, Boomker JM, Huizinga-van der Vlag A, Smedts FMM, Harmsen MC, van Luyn MJA. The use of fibrous, supramolecular membranes and human tubular cells for renal epithelial tissue engineering: towards a suitable membrane for a bioartificial kidney. *Macromolec Biosci* 2010;10(11):1345–54.
- [20] Mazzachi BC, Peake ML, Ehrhardt V. Reference range and method comparison studies for enzymatic and Jaffé creatinine assays in plasma and serum and early morning urine. *Clin Lab* 2000;46(1–2):53–5.
- [21] Luttikhuisen DT, van Amerongen MJ, de Feijter PC, Petersen AH, Harmsen MC, van Luyn MJA. The correlation between difference in foreign body reaction between implant locations and cytokine and MMP expression. *Biomaterials* 2006;27(34):5763–70.